PROCEEDINGS OF SPIE

SPIEDigitalLibrary.org/conference-proceedings-of-spie

Spatial frequency domain imaging using a snap-shot filter mosaic camera with multi-wavelength sensitive pixels

Tomas Strömberg, Rolf B. Saager, Gordon T. Kennedy, Ingemar Fredriksson, Göran Salerud, et al.

Tomas Strömberg, Rolf B. Saager, Gordon T. Kennedy, Ingemar Fredriksson, Göran Salerud, Anthony J. Durkin, Marcus Larsson, "Spatial frequency domain imaging using a snap-shot filter mosaic camera with multi-wavelength sensitive pixels," Proc. SPIE 10467, Photonics in Dermatology and Plastic Surgery 2018, 104670D (22 February 2018); doi: 10.1117/12.2289357

SPIE.

Event: SPIE BiOS, 2018, San Francisco, California, United States

Spatial frequency domain imaging using a snap-shot filter mosaic camera with multi-wavelength sensitive pixels

Tomas Strömberg*[a,b], Rolf B. Saager[b], Gordon T. Kennedy[b] , Ingemar Fredriksson[a,c], Göran Salerud[a], Anthony J. Durkin[b,d], Marcus Larsson[a]

[a]Department of Biomedical Engineering, Linköping University, 581 83 Linköping, Sweden; [b]Beckman Laser Institute and Medical Clinic, University of California, Irvine, 1002 Health Sciences Rd, Irvine, CA USA; [c]Perimed AB, Datavägen 9A, Järfälla-Stockholm, Sweden; [d]Department of Biomedical Engineering, University of California, Irvine, CA USA.

ABSTRACT

Spatial frequency domain imaging (SFDI) utilizes a digital light processing (DLP) projector for illuminating turbid media with sinusoidal patterns. The tissue absorption (μ_a) and reduced scattering coefficient (μ_s') are calculated by analyzing the modulation transfer function for at least two spatial frequencies. We evaluated different illumination strategies with a red, green and blue light emitting diodes (LED) in the DLP, while imaging with a filter mosaic camera, XiSpec, with 16 different multi-wavelength sensitive pixels in the 470-630 nm wavelength range. Data were compared to SFDI by a multispectral camera setup (MSI) consisting of four cameras with bandpass filters centered at 475, 560, 580 and 650 nm. A pointwise system for comprehensive microcirculation analysis was used (EPOS) for comparison. A 5-min arterial occlusion and release protocol on the forearm of a Caucasian male with fair skin was analyzed by fitting the absorption spectra of the chromophores HbO2, Hb and melanin to the estimated μ_a. The tissue fractions of red blood cells (f_{RBC}), melanin (f_{mel}) and the Hb oxygenation (S_{O_2}) were calculated at baseline, end of occlusion, early after release and late after release. EPOS results showed a decrease in S_{O_2} during the occlusion and hyperemia during release ($S_{O2} = 40\%$, 5%, 80% and 51%). The f_{RBC} showed an increase during occlusion and release phases. The best MSI resemblance to the EPOS was for green LED illumination ($S_{O2} = 53\%$, 9%, 82%, 65%). Several illumination and analysis strategies using the XiSpec gave un-physiological results (e.g. negative S_{O_2}). XiSpec with green LED illumination gave the expected change in f_{RBC} , while the dynamics in S_{O_2} were less than those for EPOS. These results may be explained by the calculation of modulation using an illumination and detector setup with a broad spectral transmission bandwidth, with considerable variation in μ_a of included chromophores. Approaches for either reducing the effective bandwidth of the XiSpec filters or by including their characteristic in a light transport model for SFDI modulation, are proposed.

Keywords: structured illumination, spatial frequency, modulation, diffuse light spectroscopy, multi spectral imaging, tissue optical properties

1. INTRODUCTION

Tissue optical properties, absorption (μ_a) and reduced scattering (μ_s'), can be quantified locally using spatial domain techniques, either by pointwise illumination and recording the spatially resolved diffuse reflectance or by illuminating tissue with a sinusoidal spatially varying pattern with spatial frequency f_x. The latter technique can be executed in a couple of different ways 1) by imaging a single point (~ 1 mm^2) in the illuminated field of view and using a spectrometer to resolve optical properties in the small area as a function of wavelength[1] or 2) by using a camera to image a larger area, (> 100 cm^2). The former technique is generally referred to as spatial frequency domain spectroscopy (SFDS) and the latter as spatial frequency domain imaging (SFDI). In SFDI, modulation depth as a function of f_x contrasts the tissue optical properties μ_a and μ_s', where μ_a contrast is found at relatively low f_x while μ_s' contrast is found for all f_x.[2] Spectral resolution

Photonics in Dermatology and Plastic Surgery 2018, edited by Bernard Choi, Haishan Zeng, Proc. of SPIE
Vol. 10467, 104670D · © 2018 SPIE · CCC code: 1605-7422/18/$18 · doi: 10.1117/12.2289357

can be obtained either via appropriate selection of light source of the illuminating DLP projector[3], or can be done in conjunction with the detecting camera[2].

We have developed an SFDI system based on a snap-shot 4x4 filter mosaic camera with 16 unique band pass filters in the 470 – 630 nm wavelength range. The camera sensor has a native resolution of 2048×1088 pixels, resulting in 512×272×16 (x×y×λ) sized hyper-cubes. This camera can be used for high-speed continuous-light spectral imaging or can be used in SFDI with reduced data acquisition times. However, each of the 16 band pass filters has a complex wavelength characteristic with a principal nominal peak and an additional smaller pass band in either the blue or the red wavelength range. As an example, the sensor had one filter with a main filter transmission peak at 613 nm and a second peak at 467nm at 60% of the main peak.

The aim of this study was to evaluate the XiSpec snap-shot filter mosaic sensor in an SFDI system with separate red (R), green (G) and blue (B) light emitting diodes (LEDs) as light sources in the DLP. We compare the output parameters from this device to that from an SFDI system with well-defined filter characteristics (single transmission peak) and from a point probe system that we have previously described. That system, known as the enhanced perfusion and oxygen saturation (EPOS) system[4], measures local tissue blood perfusion in absolute units and tissue fractions of red blood cells (f_{RBC}) and the Hb oxygenation (S_{O_2}). We have validated the system using liquid and solid optical phantoms regarding the μ_s', f_{RBC}, S_{O_2} and the fraction of melanin (f_{mel}).[5] Accuracy of μ_s', f_{RBC}, S_{O2} was acceptable (< 15% error), while f_{mel} errors were larger. A measurement was done on forearm skin of a Caucasian male subject with fair skin during a 5-min arterial occlusion and release protocol. During this protocol an almost complete desaturation is normally observed followed by a post occlusive hyperemic response with an S_{O_2} of about 85%.[6]

2. MATERIAL AND METHODS

2.1 The SFDI system

Four monochromatic cameras (FL3-U3-32S2M-CS, Point Grey), each equipped with a 8 mm/f1.4 Tamron lens (M118FM08) were used in the MSI Setup (Figure 1). The MSI cameras were equipped with optical band pass filters at 475 nm (±25 nm, 6 OD, Edmund Optics, #86-353), at 560 nm (±5 nm, 4 OD, Edmund Optics, #88-011), at 580 nm (± 5 nm, 4 OD, Edmund Optics, #65-161) and at 650 nm (±25 nm, 4 OD, Edmund Optics, #84-786), respectively. The cameras were placed as close as possible to each other in two rows. The additional snap-shot filter mosaic camera was a XiSpec (MQ022HG-IM-SM4X4-VIS, XIMEA (R)), having 16 wavelength-specific Fabry-Perot filters placed in a recurring 4×4 pattern overlaid on the custom CMOS-chip (Figure 1). A 16 mm lens (C Series VIS-NIR TECHSPEC, Edmund Optics, #67-714) set at f=2.8 was used. The light source was a DLP projector with RGB LEDs (Texas Instruments LCR 4500-EVM) running in video mode. Polarization filters (Edmund Optics, #86-184) where placed in front of both cameras and the DLP, rejecting specular reflections from the illuminated surface. The SFDI systems were calibrated using a custom-made polydimethylsiloxane (PDMS) large form factor (20 x 20 x 2.5 cm) optical phantom with a μ_a of 0.029 - 0.035 [mm^{-1}] almost independent of wavelength in the range 450-650 nm, and a μ_s' ranging 2.44 – 1.51 [mm^{-1}].

λ_1	λ_2	λ_3	λ_4	λ_1	λ_2	λ_3	λ_4
λ_5				λ_5			
			λ_{16}				λ_{16}

Figure 1. Photo of the SFDI systems with digital light processing projector (left) and XiSpec camera (top) and MSI cameras with 475 nm and 560 nm filter (mid row) and 650 nm and 580 nm filter (low row). Schematic showing the XiSpec filter mosaic with two 4x4 mosaics is shown to the right.

2.2 The Enhanced Perfusion and Oxygen Saturation system (EPOS)

The EPOS system, Permed AB, Järfälla, Stockholm, Sweden, has been described in detail before.[6] Briefly, it integrates diffuse reflectance spectroscopy (DRS) and laser Doppler Flowmetry (LDF) in a fiber-optic probe. The DRS unit utilizes a broadband white light source in VIS-NIR wavelength range and the LDF unit a laser light source at 785 nm. The DRS unit has an optical notch filter suppressing wavelengths 790±20 nm. The fiber-optic probe has one LDF detector fiber with a distance of 0.8 mm from the source fiber and two DRS detecting fibers at a distance of 0.4 and 1.2 mm, respectively, from the DRS source fiber.

An adaptive three-layer skin model for DRS and LDF based on Monte Carlo simulations of light transport, was used to calculate f_{RBC}, S_{O_2} and model-based perfusion. The model is described in Fredriksson et al.[4] DRS and LDF spectra were calculated from the skin model and compared to measured spectra in an optimization routine to find the skin model with the best fit to measured spectra. The microcirculatory parameters were calculated directly from the optimal model.

Absorption coefficients for reduced hemoglobin were derived from Prahl (http://omlc.ogi.edu/spectra/hemoglobin/index.html) and oxygenized hemoglobin from Zijlstra. [7] The reason for chosing different sources is that Prahls reduced spectrum agrees better with spectra from other sources,[8-10] whereas Zijlstra's oxygenyzed spectra also agrees better with those sources. Our previous experience is also that chosing the spectra in this way results in an improved model fit. The absorption spectra were scaled to correspond to a mean hemoglobin concentration of red blood cells of 345 g/l RBC.

Absorption for melanin [1/mm^{-1}] was approximated by Jacqcues (http://omlc.ogi.edu/news/jan98/skinoptics.html):

$$\mu_{a,mel}(\lambda) = 6.6 \times \lambda^{-10/3}. \quad \text{(Eq. 1)}$$

The tissue fractions of red blood cells and melanin are given for the sampling volume. A melanin tissue fraction of 0.2% in the sampling volume would thus translate into 2% tissue fraction in the epidermis if the epidermis occupies 10% of the sampling volume.

2.3 Protocol

One healthy Caucasian male subject with age 43 years and a fair skin type was included in the study after giving informed consent. The study was conformed with the Declaration of Helsinki and was approved by the regional ethics review board

at Linköping University, Sweden (Dnr 2015/392-31). The subject sat in a dark room with a pressure cuff attached around the right upper arm. The EPOS probe was placed on the volar forearm in an area apparently free from large superficial vessels. The subject was asked to minimize movement during the experiments. After a 5-min baseline period, the blood pressure cuff was inflated to a pressure of 250 mm Hg. This pressure was maintained for 5 min. It was then released and followed by a 5-min hyperemia/ recovery period.

2.4 Data recording

EPOS data were recorded at 2 Hz for 15 min. The corresponding time intervals for SFDI recordings (baseline, occlusion, early after release and late after release), started at t = 150, t = 510, t = 650 and t = 800 s, respectively.

Each SFDI recording lasted approximately 80 s with the illumination sequence RGB, R, G, and B. The spatial frequencies f_x = 0, 0.03 0.06, 0.09, 0.12 and 0.2 [mm^{-1}], were used, as has been the convention employed by other groups.[11] The hypercubes were imaged with a resolution of at least 2.4 pixels/mm (XiSpec).

The intensity detected by the XiSpec camera depends both on the XiSpec filter transmission spectra and the DLP emission spectra. As an example, the sensitivity for the three XiSpec pixels are presented in Figure 2, left panels, together with the DLP emission spectrum for the R, G and B LEDs, respectively. The weighted pixel sensitivities, calculated as the product of the filter transmission and the LED emission spectrum, are presented in Figure 2, right panel. As an example, for RGB (3 color) and B (blue alone) LED illuminations the maximal intensity for the 466 nm pixel is at 464 nm, while for R illumination it is at 623 nm. Selectively using LEDs with a limited wavelength spectrum effectively improves the weighted sensitivity of the XiSpec pixels by removing the multi-peak filter transmission characteristics. The corresponding calculation for the MSI system gave that the 475 nm camera had a maximal intensity at 464 nm for RGB illumination and at 493 nm for G LED illumination. For the 650 nm camera, the maximal intensity was at 630 nm.

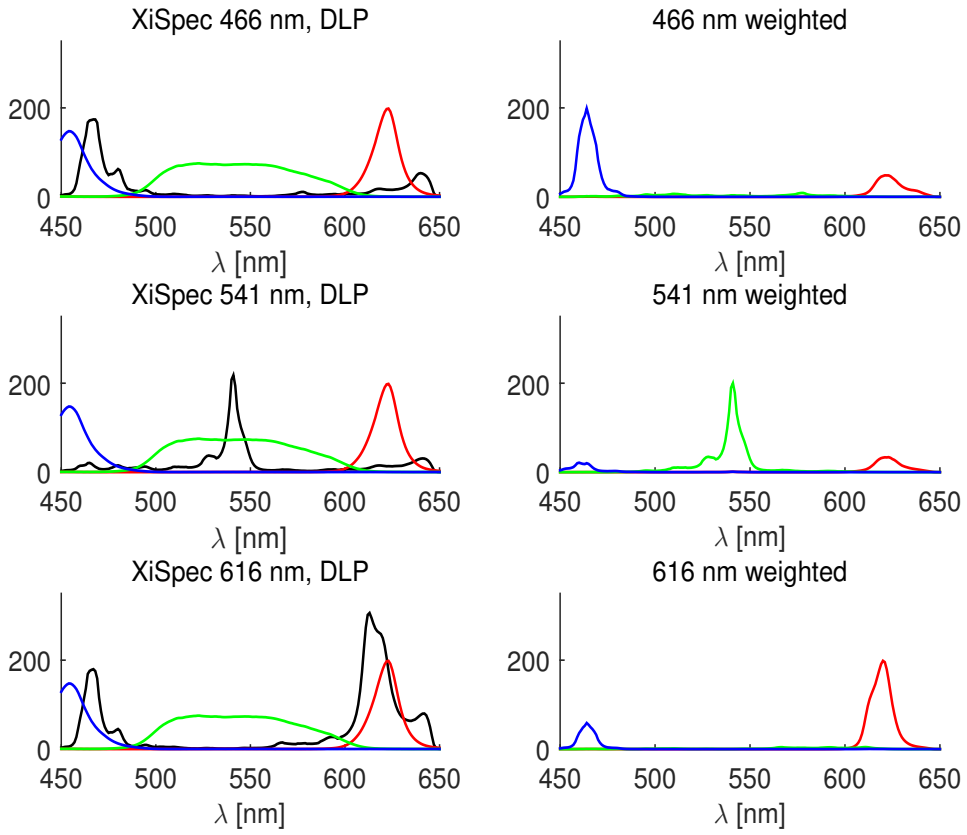

Figure 2. XiSpec spectral sensitivity for three pixels with nominal peak sensitivities at 466, 541 and 616 nm, respectively (black, left panels) and DLP LED output for R, G and B LEDs with actual current setting in the DLP (red, green and blue, respectively). XiSpec spectral sensitivity for the pixels weighted with DLP spectrum. Max peak is normalized to 200 (right panels).

2.5 Data Processing

EPOS data from these intervals was calculated as the mean value, except for early after release (~30-110 s after release), where the maximal values in that interval were calculated.[12]

The SFDI raw images for each f_x and each phase $\varphi_1 = 0$; $\varphi_2 = \frac{2\pi}{3}$; $\varphi_2 = \frac{4\pi}{3}$, were averaged to reduce noise ($I_1 = I_1(x, y, f_x, \varphi_1)$; $I_2 = I_2(x, y, f_x, \varphi_2)$; $I_3 = I_3(x, y, f_x, \varphi_3)$, before calculating the modulation (Figure 3). The modulation image $M_{obj}(x, y, f_x)$ was calculated as:[2]

$$M_{obj}(x, y, f_x) = \frac{2^{1/2}}{3}\{(I_1 - I_2)^2 + (I_2 - I_3)^2 + (I_3 - I_1)^2\}^{1/2} \quad \text{(Eq. 2)}$$

The diffuse reflectance $R_{d,obj}$ of the sample as a function of image position (x,y) and spatial frequency (f_x) was calibrated to an optical reference phantom with known optical properties, using measurements of the modulation depth, M, according to the formula[2]:

$$R_{d,obj}(x, y, f_x) = \frac{M_{obj}(x,y,f_x)}{M_{ref}(x,y,f_x)} R_{d,ref}(f_x). \quad \text{(Eq. 3)}$$

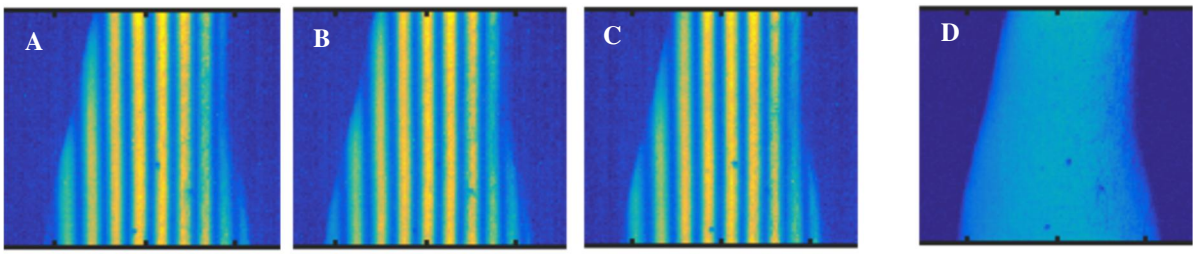

Figure 3. Forearm occlusion XiSpec camera 466 nm pixel raw images I_1, I_2, I_3 during RGB illumination with spatial frequency $f_x = 0.09$ [1/mm] and phases $\varphi = 0, \frac{2\pi}{3}, \frac{4\pi}{3}$ rad (A-C). Corresponding modulation $M_{obj}(x, y, f_x)$ image (D).

The diffuse reflectance images $R_{d,obj}(x, y, f_x)$, were spatially averaged over a region of interest marked by fiducial ink markers (Figure 4). The $R_{d,obj}$ as a function of f_x, was matched to diffuse reflectances using inverse Monte Carlo fitting. This results in μ_a and μ_s', being estimated at one wavelength depending on which MSI camera or which XiSpec filter that was used. The chromophore spectra for oxygenated and reduced hemoglobin and melanin were fitted to the measured μ_a using least-squares fitting.

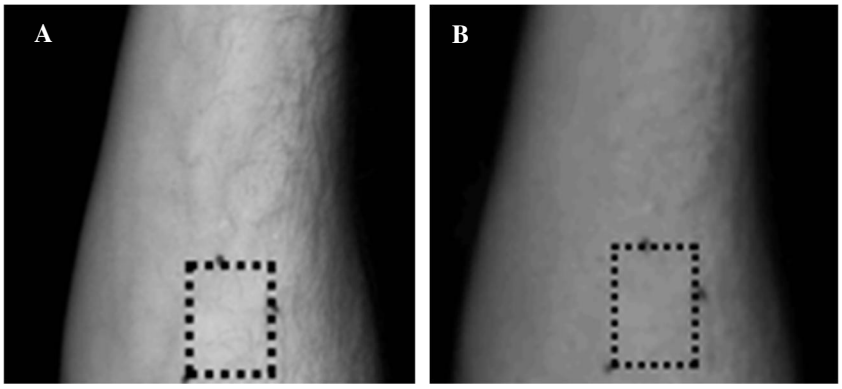

Figure 4. Forearm baseline calibrated diffuse reflectance images by MSI 650 nm camera (A) and XiSpec 466 nm pixel (B). The region of interest was selected using ink markers.

3. RESULTS

The EPOS skin recordings are shown in Figure 5 as time traces of S_{O_2} and f_{RBC}. The corresponding time intervals for SFDI recordings are marked in grey: baseline, occlusion, early after release and late after release. Note that this is not SFDI data per se, only temporal markers indicated data acquisition periods for SFDI. EPOS data from the marked intervals are presented in Table 1.

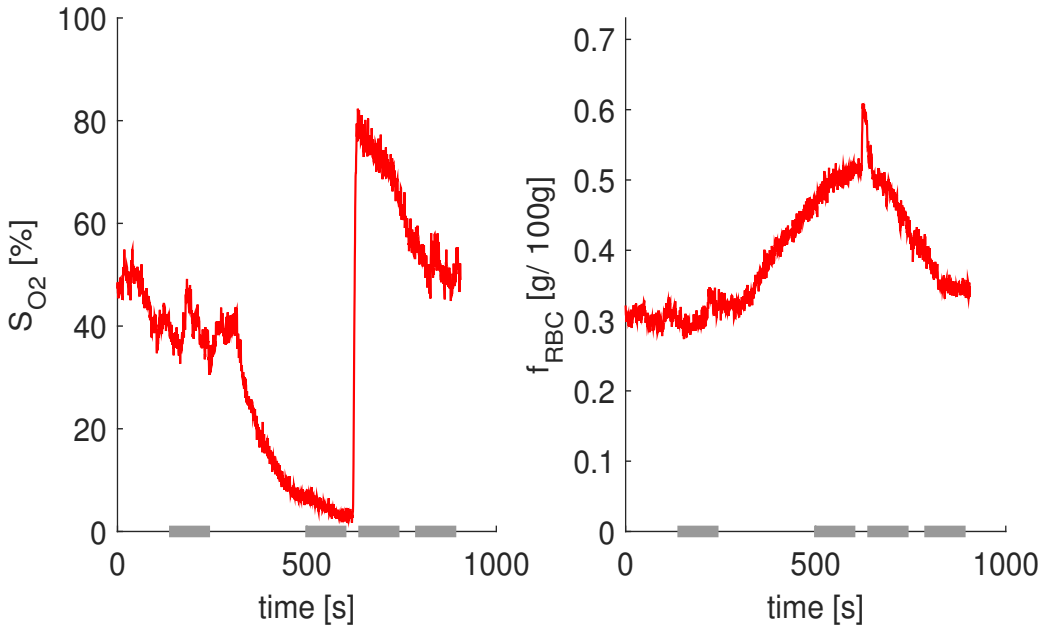

Figure 5. Skin local oxygen saturation (S_{O_2}) and fraction of RBC (f_{RBC}), as measured by EPOS system. Time intervals indicate periods with SFDI recordings: baseline, occlusion, early (~30-110 s) and late (~180-260 s) after release. Each interval lasts 80 s.

Table 1. Skin fraction of RBC (f_{RBC}), local oxygen saturation (S_{O_2}), and the fraction of melanin (f_{mel}) measured by the EPOS system and the MSI SFDI system during RGB and G LED illumination, respectively, and by the XiSpec SFDI system during G LED illumination. Phases are baseline, occlusion, early (~30-110 s) and late ~180-260 s after release of occlusion (see Material and Methods).

		Baseline	End of occlusion	~30-110 s after release	~180-260 s after release
EPOS	f_{RBC} [%]	0.30	0.50	0.52	0.36
	S_{O_2} [%]	40	4.6	80	51
MSI SFDI RGB (464, 560, 580 and 630 nm)	f_{RBC} [%]	0.24	0.34	0.43	0.29
	S_{O_2} [%]	87	40	92	93
	f_{mel} [%]	0.21	0.21	0.21	0.25
MSI SFDI RGB (560, 580 and 630 nm)	f_{RBC} [%]	0.27	0.37	0.47	0.33
	S_{O_2} [%]	42	19	64	52
	f_{mel} [%]	0.093	0.12	0.092	0.097
MSI SFDI G (493, 560 and 580 nm)	f_{RBC} [%]	0.22	0.34	0.33	0.26
	S_{O_2} [%]	53	9	82	65
	f_{mel} [%]	0.23	0.27	0.27	0.25
XiSpec SFDI G	f_{RBC} [%]	0.22	0.32	0.31	0.26
	S_{O_2} [%]	32	13	44	36
	f_{mel} [%]	0.21	0.25	0.26	0.23

SFDI data are presented in Figures 6-10 and in Table 2. Absorption coefficients μ_a from MSI and RGB illumination SFDI at the wavelengths 464, 560, 580 and 630 nm are presented in Figure 6 as asterisks. Corresponding fitted weighted

chromophore spectra at all four wavelengths and the three higher wavelengths are presented in left and right panels, respectively. Including the 464 nm wavelength in the fitting gave a better fit at 464 nm, which is expected, while fitted spectra overestimated measurements at 630 nm. Furthermore, f_{mel} was twice as high (Table 2), f_{RBC} was lower and S_{O_2} higher when including the 464 nm wavelength. Corresponding chromophore absorption spectra for the MSI RGB data for HbO2 and Hb follow the expected changes during the experiment, while the melanin spectra remains fairly constant between the different time intervals, as expected.

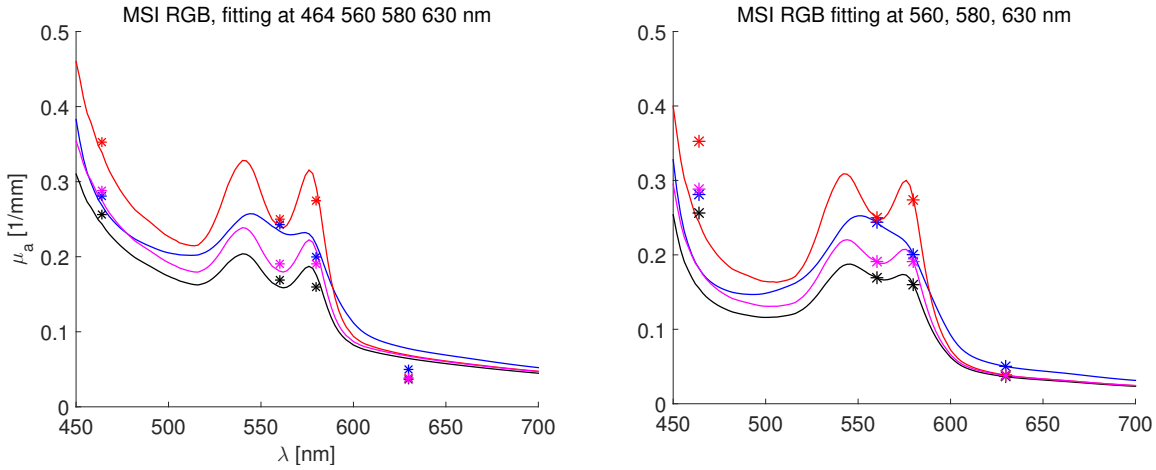

Figure 6. Tissue absorption, μ_a, by SFDI using multispectral camera imaging (MSI) during RGB LED illumination. Continuous lines show weighted HbO_2, Hb and Mel absorption spectra, with weights from fitting at all wavelengths (left) and fitting when eliminating 464 nm data (right). Black = baseline; blue = end of occlusion; red = ~30-110 s from release of occlusion; magenta = ~180-260 s after release of occlusion.

The μ_a for MSI with G LED illumination is presented in Figure 7 and Table 2. The modeled absorption spectra fits the measurements perfectly since three chromophores are fitted from three data points. The results using this configuration resembles those from the EPOS system much closer as compared with an RGB illumination scheme where the 630nm wavelength is included in the model fit.

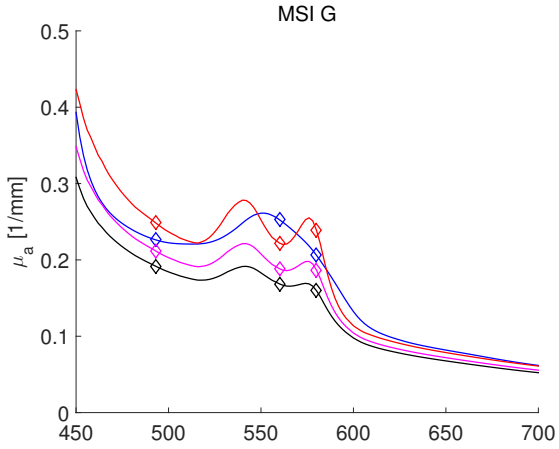

Figure 7. Tissue absorption, μ_a, by SFDI using multispectral camera imaging (MSI) during G LED illumination. Continuous lines show weighted HbO_2, Hb and Mel absorption spectra, with weights from fitting at wavelengths 493, 560 and 580 nm. Black = baseline; blue = end of occlusion; red = ~30-110 s from release of occlusion; magenta = ~180-260 s after release of occlusion.

Several configurations including the XiSpec gave non-physiological results. Fitting the three chromophore model to XiSpec data derived using either RGB or GB illumination resulted in negative HbO2/ Hb chromophore weights with either negative S_{O_2} or S_{O_2} > 100%. However, this was not the case for data from XiSpec using G LED illumination (Figure 8, Table 2). The S_{O_2} dynamic was lower with especially a low S_{O_2} at early release (44%).

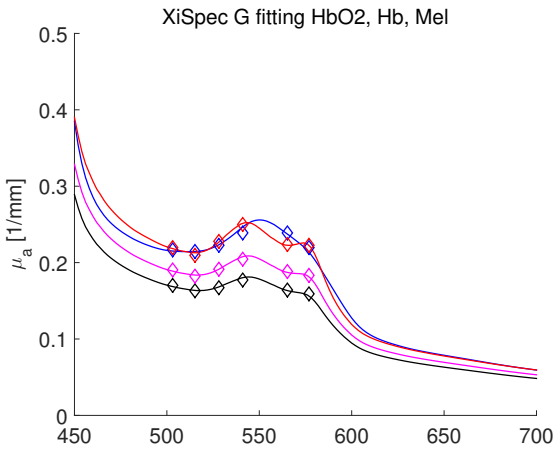

Figure 8. Tissue absorption (μ_a [1/mm]) by SFDI using XiSpec camera during G LED illumination by the DLP (left). Continuous lines show weighted HbO_2, Hb and Mel absorption spectra, with weights from fitting μ_a (see Method).

Data for reduced scattering, μ_s', estimated from MSI data using RGB illumination was comparable to that from the XiSpec using RGB illumination, while as an example data from XiSpec B LED illumination showed a higher μ_s' (Figure 9).

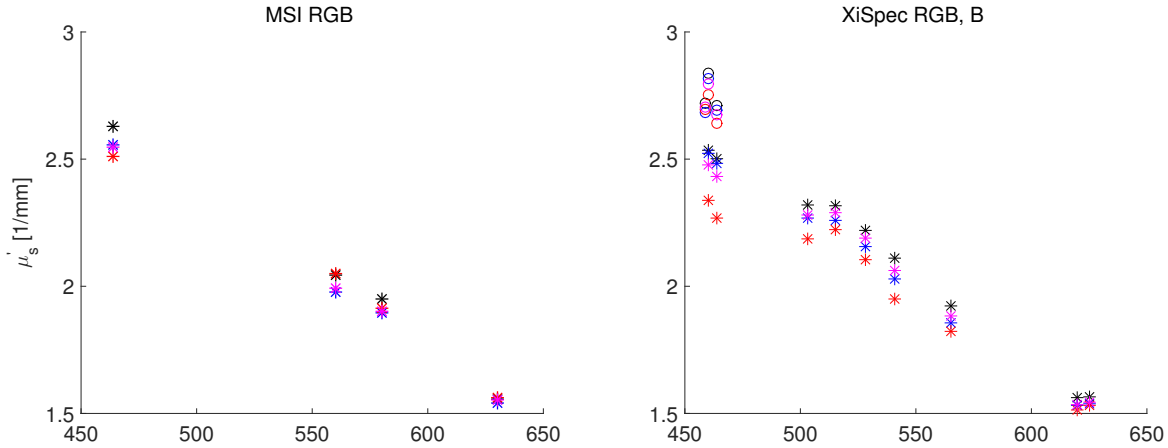

Figure 9. Reduced scattering (μ_s') by SFDI using MSI and RGB illumination and XiSpec during RGB (asterisks) and B (circle) LED illumination.

4. DISCUSSION

In this paper we have evaluated a snap-shot filter mosaic hyper spectral camera (XiSpec) with complex multi-wavelength sensitive pixels for SFDI with a DLP with RGB LEDs as light source. It was compared to a traditional multi-camera setup with bandpass filters on each camera at selected wavelengths. For comparison, a pointwise system (EPOS) for comprehensive microcirculation analysis including assessment of optical properties was used. Data were recorded on human forearm skin during well- known stimulus response caused by a 5-min arterial occlusion. The main finding was that the XiSpec camera results, because of the multiband transmission characteristics associated with each device sub-filter, depended critically on the illumination and wavelength selection. Only when applying G LED illumination, the results resembled the expected ones. We hypothesize that this was due to the improved spectral characteristics of the XiSpec filters achieved using selective LEDs.

In SFDI the diffuse reflectance of a turbid object as a function of image position (x, y) and spatial frequency (f_x) is calibrated to an optical phantom with known optical properties, using measurements of the modulation depth, M, according to Eq. 3. An inherent assumption in Eq. 3, is that this expression is valid over the wavelength used for illumination and recording. This holds for a narrow bandwidth imaging (either by the light source or by filtering the camera), but not necessarily for a wide bandwidth recording where the optical properties can vary substantially with wavelength. In the latter case, it may be less critical if the parameters on the right hand side of Eq. 3 vary less with wavelength. This is the case for the MSI 650 nm camera, which has a relatively wide bandwidth of ±25 nm. Human skin absorption varies little over this wavelength range and hence, the optical properties at the maximal sensitivity of the sensor, 630 nm, are estimated. However, the MSI 475 nm camera, with a similar filter bandwidth, will cover a range where HbO2 and Hb absorption vary approximately a factor of two (see e.g. Figure 4). Furthermore, tissue scattering will also vary more in this wavelength region. Hence, Eq. 3, will be a complex weighted sum of each entity's spectral variation. If we compare Figures 4 and 6, this camera will estimate a μ_a that varies more than 50%. The RGB illumination has a peak at 464 nm and the G illumination at 493 nm. We can, therefore, assume that this effect was causing the problems with the XiSpec sensor, where the double peak spectral sensitivity characteristics causes blurring of the finer spectral details. Therefore, it was expected that illumination by G LED lead to a better result. Possible approaches to improve this even further are: spectrally purifying the 16 filters by making linear combinations of the intensities for the different filters in order to reduce the influence of side peaks; or to include the complex filter characteristics in a light transport model of Eq. 3.

In conclusion, we have shown that using a snap-shot filter mosaic camera (XiSpec) with multi-wavelength sensitive pixels for SFDI gives results that depend critically on the DLP light source spectra. The spectral blurring caused by the complex multi-peak characteristics in the XiSpec camera hampers the estimation of Hb oxygenation. We have suggested approaches to improve the spectral resolution.

5. REFERENCES

[1] R. B. Saager, D. J. Cuccia, and A. J. Durkin, "Determination of optical properties of turbid media spanning visible and near-infrared regimes via spatially modulated quantitative spectroscopy," J Biomed Opt, 15(1), 017012 (2010).

[2] D. J. Cuccia, F. Bevilacqua, A. J. Durkin *et al.*, "Quantitation and mapping of tissue optical properties using modulated imaging," J Biomed Opt, 14(2), 024012 (2009).

[3] A. Ponticorvo, D. M. Burmeister, B. Yang *et al.*, "Quantitative assessment of graded burn wounds in a porcine model using spatial frequency domain imaging (SFDI) and laser speckle imaging (LSI)," Biomed Opt Express, 5(10), 3467-81 (2014).

[4] I. Fredriksson, O. Burdakov, M. Larsson *et al.*, "Inverse Monte Carlo in a multilayered tissue model - merging diffuse eflectance spectroscopy and laser Doppler flowmetry," J Biomed Opt, 18(12), 127004 (2013).

[5] I. Fredriksson, R. B. Saager, A. J. Durkin *et al.*, "Evaluation of a pointwise microcirculation assessment method using liquid and multilayered tissue simulating phantoms," J Biomed Opt, 22(11), 1-9 (2017).

[6] T. Stromberg, F. Sjoberg, and S. Bergstrand, "Temporal and spatiotemporal variability in comprehensive forearm skin microcirculation assessment during occlusion protocols," Microvasc Res, 113, 50-55 (2017).

[7] W. G. Zijlstra, A. Buursma, and O. W. van Assendelft, [Visible and Near Infrared Absorption Spectra of Human and Animal Haemoglobin Determination and Application] VSP Books, Utrecht, Boston, Köln,Tokyo(2000).
[8] M. K. Moaveni, [Multiple scattering field theory applied to whole blood] University of Washington, (1970).
[9] M. Cope, [The application of near infrared spectroscopy to non invasive monitoring of cerebral oxygenation in the newborn infant.] University College London, (1991).
[10] S. Takatani, and M. D. Graham., "Theoretical Analysis of Diffuse Reflectance from a Two-Layer Tissue Model," IEEE Transactions on Biomedical Engineering, 26(12), 656-664 (1979).
[11] R. B. Saager, A. Sharif, K. M. Kelly *et al.*, "In vivo isolation of the effects of melanin from underlying hemodynamics across skin types using spatial frequency domain spectroscopy," J Biomed Opt, 21(5), 57001 (2016).
[12] H. Jonasson, S. Bergstrand, F. H. Nystrom *et al.*, "Skin microvascular endothelial dysfunction is associated with type 2 diabetes independently of microalbuminuria and arterial stiffness," Diab Vasc Dis Res, 14(4), 363-371 (2017).